

Determination of Geomechanical Properties of a typical Niger Delta Reservoir Rock Using Geophysical Well Logs

Davies, Dein Honour*; Davies, Onengiyeofori Anthony; Horsfall, Opiriyabo Ibim

Physics Department, Rivers State University, Port Harcourt, Nigeria.

Article Received: 30 August 2018

Article Accepted: 29 December 2018

Article Published: 15 March 2019

ABSTRACT

In this work, we determined the geomechanical properties of a typical hydrocarbon well within the Niger Delta Basin using geophysical well logs. Geomechanical properties we estimated using acoustic velocities derived from interval transit time which was obtained from the well logs. The results obtained shows that down the well, there is a general increase in trend of Young's modulus (E), unconfined compressive strength (UCS), bulk modulus (K) and shear modulus (G) down the well, while Poison ration decreases as we go down the well. The average values obtained form E , UCS , K , G , and ν are $3.72 \times 10^9 Pa$, $3.56 \times 10^9 Pa$, $2.68 \times 10^9 Pa$, $1.48 \times 10^9 Pa$, and 0.3732 respectively.

1. INTRODUCTION

A proper understanding of geomechanics is needed to proffer solutions to reservoir compaction and subsequent surface subsidence resulting from previous oil and gas exploratin within any petroleum system. In developing a geomechanical earth model, there is need to identify and estimate some important geomechanical/poromechanical parameters. The values of these parameters are not readily available for a typical Niger Delta reservoir system, hence requiring some authors to use approximate values from reservoirs in Europe and America with similar characteristics as that of the Niger Delta basin, or standard values which may sometimes lead to slightly erroneous results, or results that may not be completely reflective of the typical Niger Delta reservoir. This is true especially in the academic sector where well log data, seismic data and relevant software may not be available. There is therefore, the need to calculate or have an estimate of the geomechanical parameters in building a geomechanical earth model, or at least have an estimate of the stress/pressure distribution within a Niger Delta reservoir system. There are diverse ways of estimating the needed properties, depending on the available data set. Sometimes, the properties can be estimated using empirical correlations (Horsrud, 2001), using acoustic velocities derived from interval transit time of well log data (Sharma & Arya; Eyinla & Oladunjoye, 2014). Although one can infer some of these properties directly from seismic or a combination of seismic and well log data (Słota-Valim, 2013). Hsu et al. (2012) used a nonlinear poroelastic model to estimate some elastic and hydraulic parameters assuming an incompressible soil grain and obtained fantastic results useful for both geomechanical, mining and groundwater engineering. Similar works have been carried out by authors, using well logs to determine rocks mechanical properties (Karacan, 2009; Archer & Rasouli, 2012; Eyinla & Oladunjoye, 2014). In order to build a geomechanical model, there is need for a proper estimation of the poromechanical properties of the reservoir under consideration. In order to do this, we need to evaluate the shale sections which are seldom available.

CITE THIS ARTICLE: Davies, Dein Honour; Davies, Onengiyeofori Anthony; Horsfall, Opiriyabo Ibim, "Determination of Geomechanical Properties of a typical Niger Delta Reservoir Rock Using Geophysical Well Logs", *Asian Journal of Applied science and Technology*, Volume 3, Issue 1, Pages 222-233.

Horsrud (2001) carried out an extensive study on shales, mainly from the North Sea to establish some correlations that will enable us predict the static mechanical properties of shale from sources such as sonic log and acoustic measurements using the shale principal wave velocity. Geomechanical modelling of reservoir, source rocks and seals have been carried out by numerous authors using well logs derived parameters and other methods (Grazulis, 2016).

2. THEORETICAL BACKGROUND

Geomechanical properties of rocks are either statically or dynamically measured. Static measurement involves principally the use of core specimens in the laboratory, where the core specimens are exposed to incremental compression until they undergo fracture while recording the stress-strain curve, such that the required mechanical properties can be estimated numerically from the stress-strain curve. On the other hand, dynamic mechanical properties can be obtained using p-wave velocities obtained from seismic, well logs or laboratories-analyzed core data (Al-Shayea, 2004; Hongzhi, 2005; Chang et al., 2006; Xu et al., 2016). To avoid numerous drilling problems, relative to wellbore stability or pore pressure-induced problems, scientist and engineers will need to precisely describe the geomechanical properties of a rock. This can be achieved by numerically describing the stress and mechanical properties of the rocks for a given stratigraphic section of the geologic field or basin of interest. Hence, beginning from the 1950s, sonic and density logs were employed by geophysics, geosciences and others in determining the dynamic mechanical properties of a reservoir rock which include bulk modulus, young modulus Poisson's ratio and shear modulus, which can then be converted to static mechanical properties, which can thereafter be used to estimate rock strength properties (Archer & Rasouli, 2012; Najibi et al., 2015; Xu et al., 2016). Typically, dynamic moduli values are usually less than their equivalent static moduli, and as such the ratio of dynamic moduli to static moduli gets smaller with increasing confining pressures, while their difference increases in tight sands and shale reservoirs (Adham, 2016).

In this paper, we will focus on obtaining dynamic rock mechanical properties beginning from sonic log by converting the compressional interval transit time, Δt_p^{-1} to p-wave velocities and then applying well established empirical relations, estimate the static mechanical properties as well (Archer & Rasouli, 2012; Słota-Valim, 2013, 2015; Jamshidian et al., 2017). The obvious advantage of this method over measurement of static properties directly, using uniaxial loading test is that it is less destructive to the specimen, more cost effective and time efficient (Zhang & Bentley, 2005). The p-wave, v_p and s-wave, v_s , velocities are the inverse of interval transit times (Brandás, 2012; Horsfall et al., 2013, 2014; Schön, 2015).

$$V_p = \Delta t_p^{-1} \quad (1)$$

$$V_s = \Delta t_s^{-1} \quad (2)$$

Accurate reservoir geomechanical behavior can aid in the prediction of production and restitution rates of hydrocarbon reservoirs (Bemer et al., 2001). Rock mechanical responses are greatly influenced by the presence of

freely moving fluids in the rock, either as a result of induced increase in dilation by pore pressure or, by rock compression induced pore pressure increase, especially where the fluid cannot escape from the pore network, as seen in shales and shaley formations (Detournay & Cheng, 1993; Kumer et al., 2012; Hassanzadan, 2013). Hence, the justification to begin computation from interval transit time. P-wave velocity is a function of the rocks' mechanical properties and is therefore proportional to the strength of the rock, while the s-wave velocity which depends on the matrix composition and microstructure as well as the pore network and pore fluid distribution is inversely proportional to the strength of the material (Eyinla & Oladunjoye, 2014). Principally, the well log suite compressional interval transit time, thus s-wave velocity can be obtained using Greenberg and Castagna (1992) correlations for shales and shaley sandstones (Mavko et al., 2009; Horsfall et al., 2014).

$$(V_{s-sand} = 0.80416 V_p - 0.85588)km/s \quad (3)$$

$$(V_{s-shale} = 0.76969 V_p - 0.86735)km/s \quad (4)$$

3. METHODOLOGY

Beginning from Hooke's law, external stress applied per unit area is proportional to the resulting fractional deformation (strain), there are three (3) possible types of deformation described by different elastic moduli depending on the manner in which the external force is applied to the material under investigation. The moduli are Young's, bulk and shear moduli. While Young's modulus measures a materials ability or inability thereof to undergo elastic deformation, the strength of a material is defined by either the bulk modulus or the shear modulus (Archer & Rasouli, 2012; Eyinla & Oladunjoye, 2014).

Young's modulus (E): This is the extensional stress to the extensional strain ratio in a uniaxial stress state (Mavko et al., 2009). Assuming there is no change in the orthogonal normal stresses, the ratio of incremental normal stress to its resultant strain gives the Young's modulus for any mechanical body (Bjørlykke et al., 2015)

$$E = \frac{F/A}{dl/l} \quad (5)$$

$$E = \frac{\sigma_{zz}}{\epsilon_{zz}} \quad (6)$$

where, $\sigma_{zz}/\epsilon_{zz}$ are the principle normal stress and the compressive strain respectively in the z-direction.

In order to determine static and dynamic Young's modulus we can begin the ratio of axial stress σ to axial strain ϵ_a ,

$$E = \frac{\sigma}{\epsilon_a} \quad (7)$$

As was mentioned earlier, there exist a relationship between v_s, v_p and the elastic moduli. Dynamic Young's modulus can be obtained from elastic wave velocity from well logs (Archer & Rasouli, 2012; Eyinla & Oladunjoye, 2014; Jamshidian et al., 2017);

$$E_{dyn} = \frac{\rho V_s^2 (3V_p^2 - 4V_s^2)}{(V_p^2 - V_s^2)} \quad (8)$$

And static Young's modulus, typically determined from deformation experiments in the laboratory, we can substitute the following equations by Wang and Nur (2000) as cited in (Mavko et al., 2009)

$$E_{stat} = 0.4145E_{dyn} - 1.0593 \quad (\text{For soft rocks; } E_{stat} < 15\text{GPa}) \quad (9)$$

$$E_{stat} = 1.153E_{dyn} - 15.2 \quad (\text{For hard rocks; } E_{stat} > 15\text{GPa}) \quad (10)$$

The bulk modulus, K is the extent or measure of a substance's resistance to isotropic squeezing. A material subjected to an isotropic pressure from P_1 to pressure P_2 will compress from its initial volume v_1 to a new smaller volume v_2 . The ratio of the increase in pressure to the resulting volumetric decrease gives the bulk modulus of the substance thus;

$$K = \frac{P_2 - P_1}{(v_1 - v_2)/v_1} = \frac{\Delta P}{\Delta v/v} \quad (11)$$

Bulk modulus, K , is the change in volume under hydrostatic stress σ_0 (Brinson & Brinson, 2008; Fjar et al., 2008).

$$K = \frac{\sigma_0}{\epsilon_{xx}} = \frac{1}{3} \frac{\sigma_{xx}}{\epsilon_{xx}} \quad (12)$$

$$K = \frac{\Delta\sigma}{\epsilon_{vol}} = \lambda + \frac{2}{3}G \quad (13)$$

Gases are easily compressed, while solids and liquid are only compressed with difficulty. It is the reciprocal of compressibility β .

$$\beta = \frac{1}{K} \quad (14)$$

For an isotropic material (Bjørlykke et al., 2015),

$$K = \frac{E}{3} (1 - 2\nu) \quad (15)$$

We can compute the dynamic bulk moduli with the following relationship obtained from velocity and density data (Jizba, 1992; Brinson & Brinson, 2008; Mavko et al., 2009; Archer & Rasouli, 2012)

$$K_{dyn} = \rho \left(V_p^2 - \frac{4}{3} V_s^2 \right) \quad (16)$$

$$K_{sta} = \frac{E_{sta}}{3(1 - 2\nu_{sta})} \quad (17)$$

The shear modulus, G is the degree to which a material can be subjected to a shearing stress and still resist shearing. Just like bulk modulus, dynamic shear modulus can be estimated from density measurements and sonic velocities (Mavko et al., 2009; Eyninla & Oladunjoye, 2014). The importance of shear modulus cannot be overemphasized when comparing the strength of different geologic formations.

$$G_{dyn} = \rho V_s^2 \quad (18)$$

$$G_{stat} = \frac{E_{sta}}{2(1 + \nu_{sta})} \quad (19)$$

Poisson Ratio ν

Poisson's ratio is the measure longitudinal contraction due to lateral elongation caused by the application of a uniaxial stress (Fjar et al., 2008). Like other mechanical properties can be used to predict geomechanical behavior of rock formations and is therefore affected by production- or injection-induced reservoir volume changes (Zhang & Bentley, 2005).

$$\nu = -\frac{\varepsilon_y}{\varepsilon_x} = \frac{\lambda}{2(\lambda + G)} = \frac{3K - 2G}{2(3K + G)} \quad (20)$$

According to Burshtein (1968), dynamic Poisson ratio can be obtained using the resonance method above or the pulse test method involving the use of sonic velocities, but the later gives more accurate results. The pulse test method was also used by (Fjar et al., 2008; Mavko et al., 2009; Archer & Rasouli, 2012).

$$\nu_{dyn} = \frac{V_p^2 - 2V_s^2}{2(V_p^2 - V_s^2)} \quad (21)$$

Fei et al. (2016) using both static methods (using core data) and dynamic method (sonic velocities) showed that there is no obvious relationship between static and dynamic Poisson ratio. For this paper, we assume that $\nu_{sat} = \nu_{dyn}$

Unconfined Compressive Strength UCS.

Formation compressive strength and tensile strength typically increases with increasing rock density and decreasing rock porosity as they are both closely related to rock mineralogy and porosity distribution (Xu et al., 2016)

UCS can be estimated either by static method by applying uniaxial or compressive stress to a core specimen until fracture occurs, it can also be predicted dynamically from sonic log data-derived E_{sta} , E_{dyn} or V_p depending on the availability of data (Mavko et al., 2009; Najibi et al., 2015). However, according to Najibi et al. (2015), estimating UCS from E_{dyn} gives a more accurate value compared to that obtained using V_p or E_{sta} . Just like other mechanical properties defined above, UCS can be used in the estimation of in situ stress, reservoir compaction, stability

analysis of reservoir wellbore, and other geomechanical characteristics of geologic formations, and is derived in this paper using empirical correlation by (Chang et al., 2006).

$$UCS = 2.28 + 4.1089E_{dyn} \quad (24)$$

3.1 Results and Discussions

Several wells were delineated for the purpose of this research; however, results are only presented for one well as the results obtained for all the wells are similar. The well is about 11,000 ft (~3,000m) deep and has just two (2) major reservoirs, separated by shaley caprock/seal. Reservoir 1 is principally oil, while reservoir 2 is a composite of oil and water. Below, the table shows the column statistics showing minimum and maximum values of the geomechanical properties as well as the mean values. The mean, minimum and maximum of the geomechanical properties are shown below.

Table 1: Column Statistics of the well

	E_{sta} (Pa)	K_{sta} (Pa)	G_{sta} (Pa)	UCS (Pa)	ν_{dyn}
Number of values	967	967	967	967	967
Minimum	1.45×10^9	1.93×10^9	5.16×10^8	1.44×10^{10}	0.3016
Maximum	6.96×10^9	3.31×10^9	3.14×10^9	6.90×10^{10}	0.4203
Mean	3.72×10^9	2.68×10^9	1.48×10^9	3.68×10^{10}	0.3732

Below is the distribution of geomechanical properties downhole of the well, separated top and bottom of reservoir zones and shaley seals/caprock zones.

Table 2: Distribution of mechanical properties, top and bottom, downhole of formation zones

Well 2		ν_p (m/s)	ν_s (m/s)	MD (m)	E_{sta} (Pa)	UCS (Pa)	K_{sta} (Pa)	G_{sta} (Pa)	ν_{sta}
Caprock 1	Top	2659.29	1179.48	2091.39	3.54×10^9	3.51×10^{10}	2.48×10^9	1.40×10^9	0.3775
	Bottom	2730.74	1234.48	2174.44	4.05×10^9	4.02×10^{10}	2.84×10^9	1.61×10^9	0.3715
Reservoir (oil)	Top	2643.29	1269.75	2174.60	4.22×10^9	4.19×10^{10}	2.66×10^9	1.71×10^9	0.3500

	Bottom	2577.37	1216.74	2188.46	3.52 $\times 10^9$	3.49 $\times 10^{10}$	2.11 $\times 10^9$	1.44 $\times 10^9$	0.3566
Seal/caprock	Top	2568.12	1109.31	2188.62	3.02 $\times 10^9$	2.99 $\times 10^{10}$	2.20 $\times 10^9$	1.18 $\times 10^9$	0.3853
	Bottom	2599.20	1133.23	2217.12	3.41 $\times 10^9$	3.38 $\times 10^{10}$	2.68 $\times 10^9$	1.32 $\times 10^9$	0.3826
Reservoir (oil)	Top	2745.23	1351.72	2217.27	4.63 $\times 10^9$	4.59 $\times 10^{10}$	2.58 $\times 10^9$	1.93 $\times 10^9$	0.3399
	Bottom	2857.06	1441.66	2232.36	4.99 $\times 10^9$	4.94 $\times 10^{10}$	2.41 $\times 10^9$	2.16 $\times 10^9$	0.3292
Reservoir (gas)	Top	2839.42	1427.47	2232.51	4.93 $\times 10^9$	4.89 $\times 10^{10}$	2.43 $\times 10^9$	2.12 $\times 10^9$	0.3309
	Bottom	2958.62	1523.32	2238.60	6.01 $\times 10^9$	5.95 $\times 10^{10}$	2.92 $\times 10^9$	2.60 $\times 10^9$	0.3196

The results obtained shows that all through the well, $E > UCS > K > G$. Below is a representation of the results obtained by plotting a graph of the geomechanical properties against the mean depth (MD) for each caprock/seal and reservoir sections of the well using Microsoft Excel.

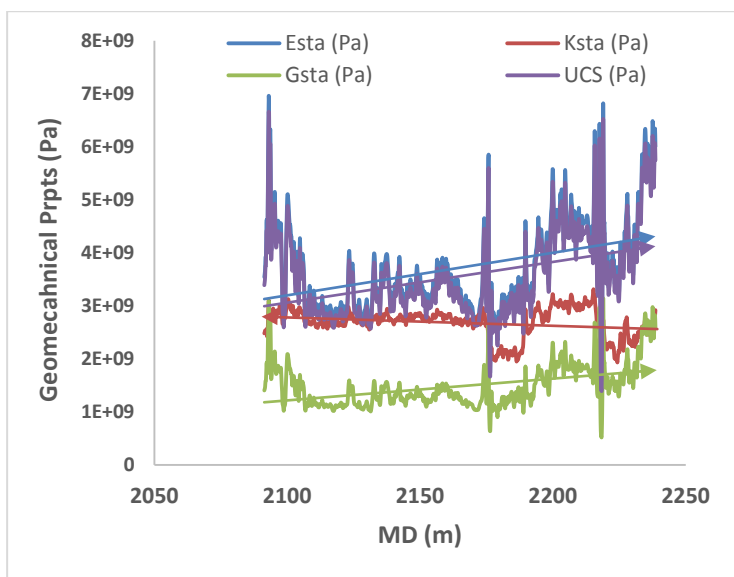


Figure 1: Geomechanical Properties (Pa) vs. MD (m) down the well

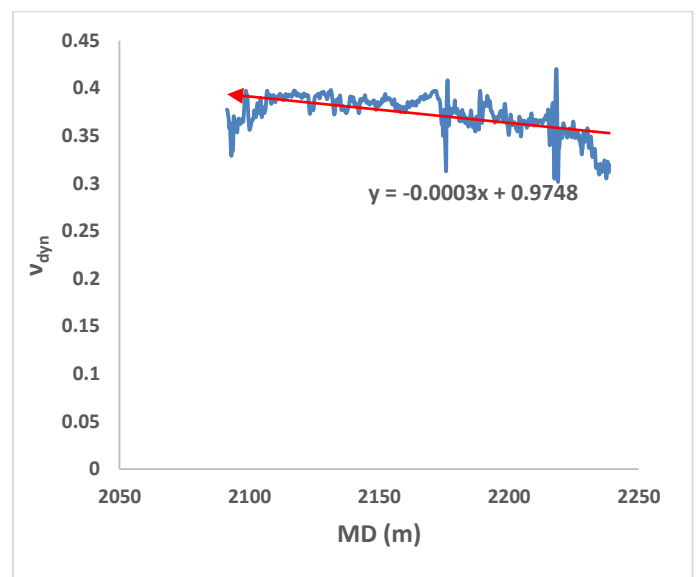


Figure 2: Poisson ratio vs. MD for Well 2

Figure 1 shows that the variation of the geomechanical properties is similar to that of the sonic velocities from which they are calculated. The values of these properties increase at deeper depths, which is most likely due to the magnitude of the overburden and increased compaction, as is depicted by the increasing sonic velocities. These geomechanical properties vary differently within various formations. The results are different for Poisson ratio, as seen in Figure 3, which generally decreases with increasing depth, therefore indicating more overburden as we go further downhole. Within the transition zones however, we can observe very significant variation in geomechanical properties compared to the values of same within reservoir and caprock zones.

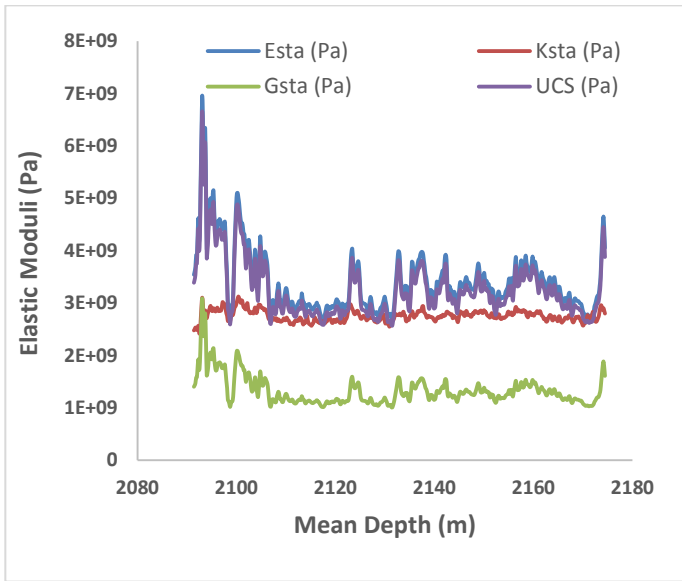


Figure 4: Variation of Geomechanical properties with depth within Caprock

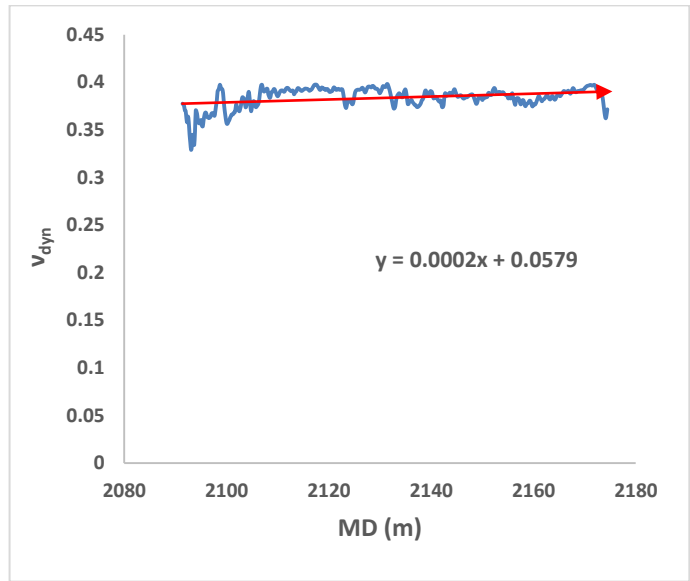


Figure 5: Variation of Poisson ratio with depth within Caprock

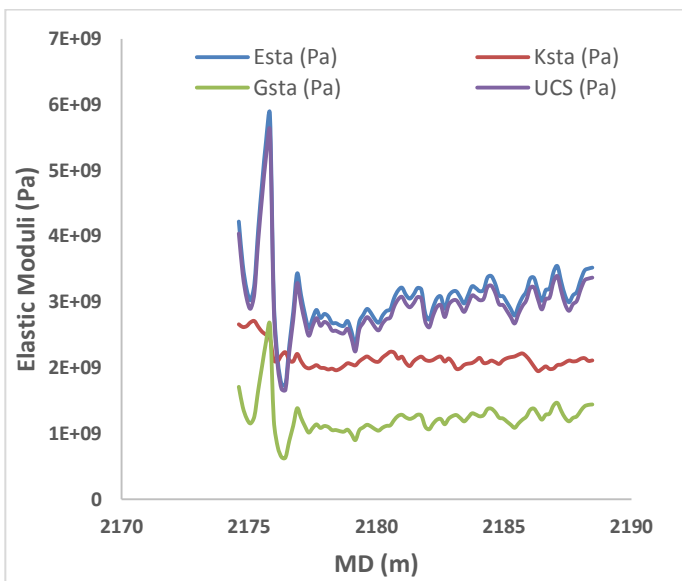


Figure 6: Variation of Geomechanical properties with depth within reservoir 1 (Oil)

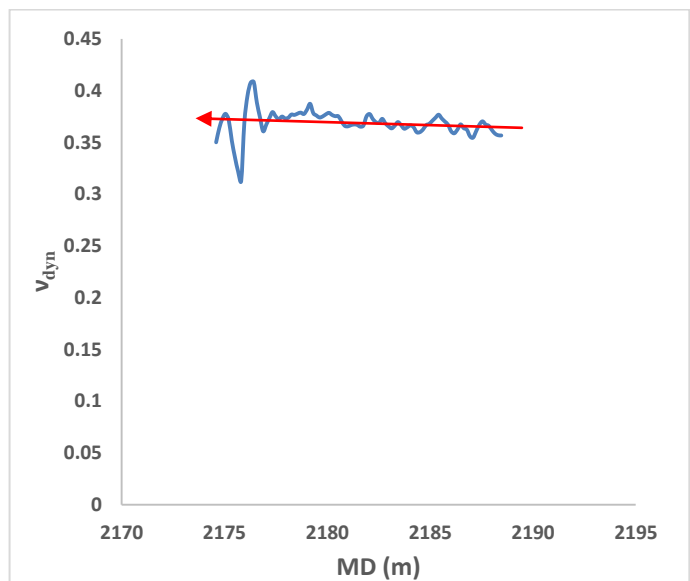


Figure 7: Variation of Poisson ratio with depth within reservoir 1 (oil)

Within the caprock zone, which is principally shale, there is only a slight increase in the geomechanical properties as we go downhole, as seen in *Figure 3*. The slight variations observed could be as a result of the clay minerals/fluid within the caprock. Observe the kink around 2090m, which is a transition zone from sandstone to shale. As shown in *Figure 5*, apart from the kink observed in the transition zone from shale to reservoir sandstone, the geomechanical properties within this reservoir sandstone zone only varies slightly, with Poisson ratio decreasing with increasing depth, and other elastic properties increasing slightly with increasing depth.

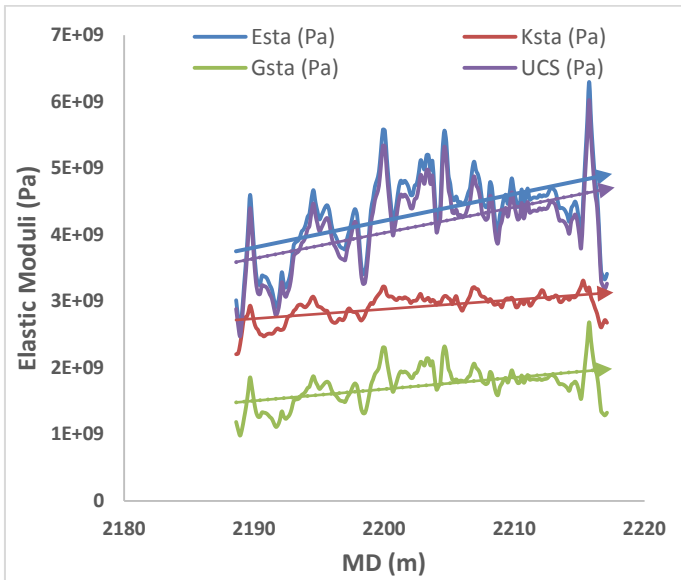


Figure 8: Variation of Geomechanical properties with depth within Caprock/Seal separating the two reservoirs

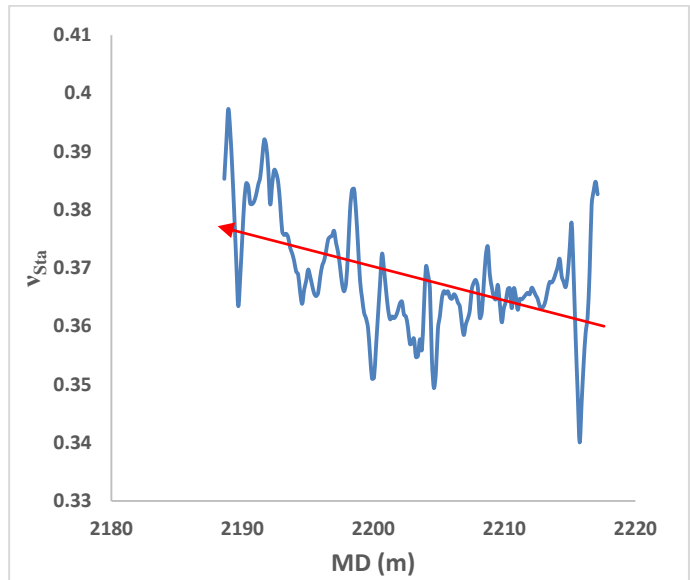


Figure 9: Variation of Poisson ratio with depth within Caprock/Seal separating the two reservoirs.

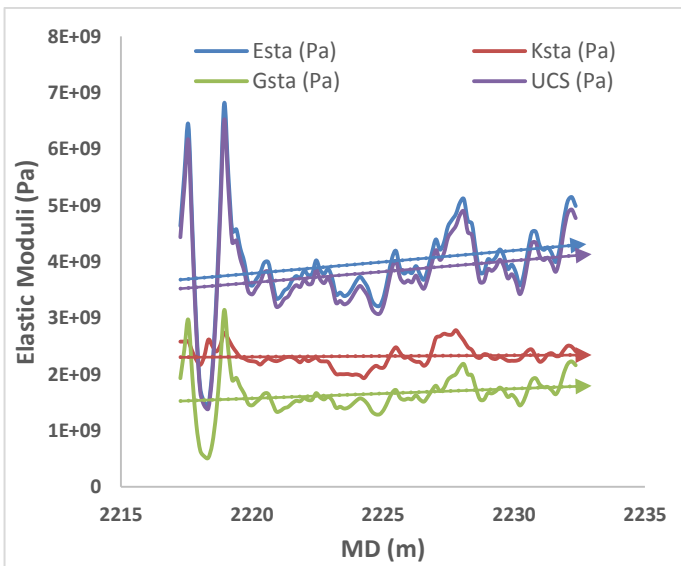


Figure 10: Variation of geomechanical properties with depth within reservoir 2 (oil zone)

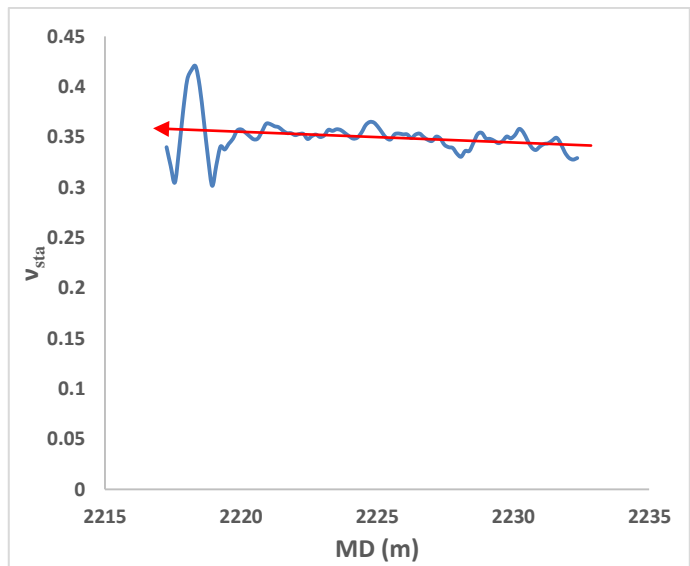


Figure 11: Variation of Poisson ratio with depth within reservoir 1 (oil zone).

Within this reservoir (oil) zone, geomechanical properties are relatively constant with only a slight change, observed in the variation of Poisson ratio with depth, which appears to decrease with increasing depth (as shown in Figures 9 and 10).

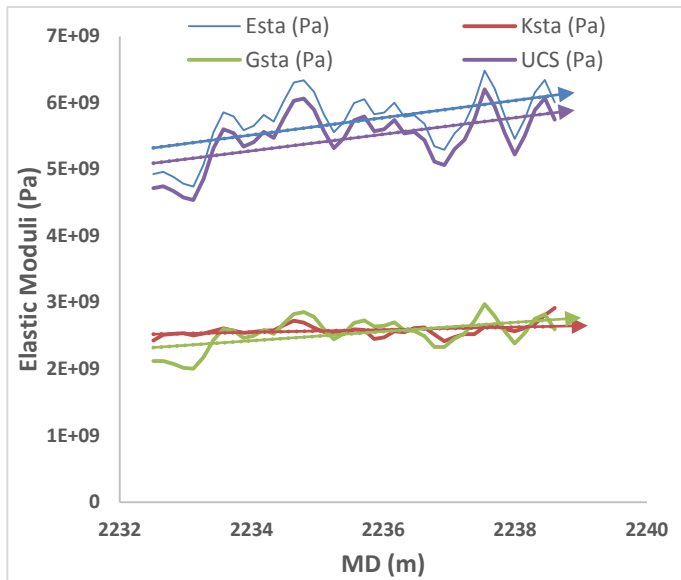


Figure 12: Variation of geomechanical properties with depth within reservoir 2 (gas zone)

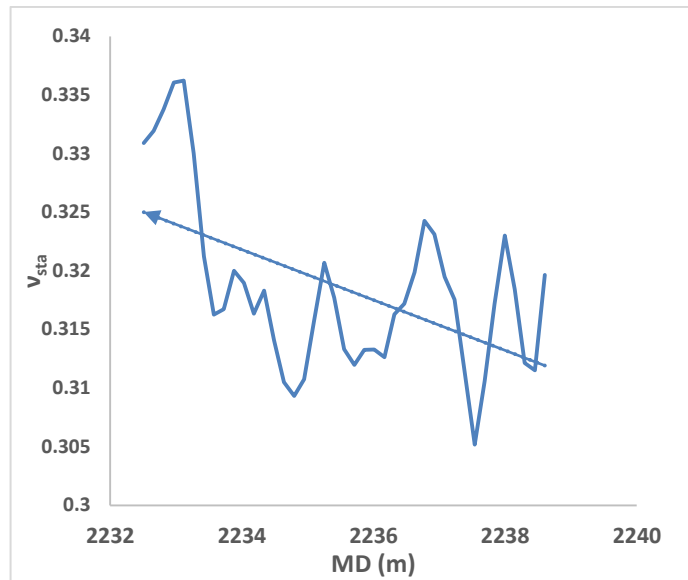


Figure 13: Variation of Poisson ratio with depth within reservoir 1 (gas zone)

The change in Poisson ratio with depth within this reservoir (gas) zone is very obvious. From Figures 11 and 14 it can be seen that while Poisson ratio is decreasing remarkably with increasing depth, other geomechanical properties are increasing with increasing depth.

3.2 CONCLUSION

Generally, as we go down the well in any formation, overburden increases. The increase in overburden leads to a decrease in porosity and thus formation compaction. This is evidenced by the increase in Young's modulus (E_{sta}), Unconfined Compressive Strength (UCS) Bulk modulus and Shear modulus. This implies that as we go deeper, the formation become more difficult to compress or twist by the application of external pressure, i.e. the less likely the formation appears to undergo deformity, except by the application of stresses larger than estimated above. Poisson ratio on the other hand, decreases with increasing depth, i.e. the less likelihood of the formation contracting.

REFERENCES

- Adham, A. (2016). Geomechanics model for wellbore stability analysis in field" X" North Sumatra Basin. (PhD), Colorado School of Mines. Arthur Lakes Library.
- Al-Shayea, N. A. (2004). Effects of testing methods and conditions on the elastic properties of limestone rock. *Engineering geology*, 74(1-2), 139-156.
- Archer, S., & Rasouli, V. (2012). A Log Based Analysis To Estimate Mechanical. *Petroleum And Mineral Resources*, 163-170.
- Bemer, E., Boutéca, M., Vincké, O., Hoteit, N., & Ozanam, O. (2001). Poromechanics: From Linear to Nonlinear Poroelasticity and Poroviscoelasticity. *Oil & Gas Science and Technology – Rev. IFP*, 56(6), 531-544.

- Bjørlykke, K., Høeg, K., & Mondol, N. H. (2015). Introduction to Geomechanics: stress and strain in sedimentary basins *Petroleum Geoscience* (pp. 301-318): Springer.
- Brandås, L. T. (2012). Relating acoustic wave velocities to formation mechanical properties. Institutt for petroleumsteknologi og anvendt geofysikk.
- Brinson, H., & Brinson, C. (2008). Stress and strain analysis measurement *Polymer engineering science and viscoelasticity: an introduction*: New York: Springer.
- Burshtein, L. (1968). Determination of poisson's ratio for rocks by static and dynamic methods. *Journal of Mining Science*, 4(3), 235-238.
- Chang, C., Zoback, M. D., & Khaksar, A. (2006). Empirical relations between rock strength and physical properties in sedimentary rocks. *Journal of Petroleum Science and Engineering*, 51(3-4), 223-237.
- Detournay, E., & Cheng, A. H.-D. (1993). Fundamentals of Poroelasticity. *Comprehensive Rock Engineering: Principles, Practice and Projects*, 2, 113-171.
- Eyinla, D. S., & Oladunjoye, M. A. (2014). Estimating geo-mechanical strength of reservoir rocks from well logs for safety limits in sand-free production. *J Environ Earth Sci*, 4(20), 38-43.
- Fei, W., Huiyuan, B., Jun, Y., & Yonghao, Z. (2016). Correlation of Dynamic and Static Elastic Parameters of Rock. *Electronic Journal of Geotechnical Engineering*, 21(4), 1551-1560.
- Fjar, E., Holt, R. M., Raaen, A., Risnes, R., & Horsrud, P. (2008). *Petroleum related rock mechanics* (Vol. 53): Elsevier.
- Grazulis, A. K. (2016). Analysis of stress and geomechanical properties in the Niobrara Formation of Wattenberg Field, Colorado, USA. Colorado School of Mines. Arthur Lakes Library.
- Greenberg, M. L., & Castagna, J. P. (1992). Sheer-Wave Velocity Estimation in Porous Rocks: Theoretical Formulation, Preliminary Verification and Application. *Geophysical Prospecting*, 40(2), 195-209.
- Hassanzadan, A. (2013). Thermomechanical and poromechanical behavior of Flechtinger sandstone. (PhD), University of Berlin. (D 83)
- Hongzhi, L. B. B. (2005). Advances in Calculation Methods for Rock Mechanics Parameters [J]. *Petroleum Drilling Techniques*, 5, 011.
- Horsfall, O., Omubo-Pepple, V., & Tamunobereton-ari, I. (2013). Correlation analysis between sonic and density logs for porosity determination in the south-eastern part of the Niger Delta Basin of Nigeria. *Asian Journal of Science and Technology*, 4(03), 001-005.
- Horsfall, O., Omubo-Pepple, V., & Tamunobereton-ari, I. (2014). Estimation of Shear Wave Velocity for Lithological Variation in the North-Western Part of the Niger Delta Basin of Nigeria. *American Journal of Scientific and Industrial Research*, 5(1), 13-22.
- Horsrud, P. (2001). Estimating mechanical properties of shale from empirical correlations. *SPE Drilling & Completion*, 16(02), 68-73.
- Hsu, K.-C., Wang, S.-J., & Wang, C.-L. (2012). Estimating poromechanical properties using a nonlinear poroelastic model. *Journal of Geotechnical and Geoenvironmental Engineering*, 139(8), 1396-1401.
- Jamshidian, M., Mansouri Zadeh, M., Hadian, M., Nekoeian, S., & Mansouri Zadeh, M. (2017). Estimation of minimum horizontal stress, geomechanical modeling and hybrid neural network based on conventional well logging data—a case study. *Geosystem Engineering*, 20(2), 88-103.
- Jizba, D. L. (1992). Mechanical and acoustical properties of sandstones and shales. (PhD), Stanford University.
- Karacan, C. Ö. (2009). Elastic and shear moduli of coal measure rocks derived from basic well logs using fractal statistics and radial basis functions. *International Journal of Rock Mechanics and Mining Sciences*, 46(8), 1281-1295.
- Kumer, V., Saluja, H., & Kumar, D. (2012). Static fields produced by point sources in porous media. *Far East Journal of Applied Mathematics*, 63(2), 73-80.
- Mavko, G., Mukerji, T., & Dvorkin, J. (2009). *The rock physics handbook: Tools for seismic analysis of porous media*: Cambridge university press.
- Najibi, A. R., Ghafoori, M., Lashkaripour, G. R., & Asef, M. R. (2015). Empirical relations between strength and static and dynamic elastic properties of Asmari and Sarvak limestones, two main oil reservoirs in Iran. *Journal of Petroleum Science and Engineering*, 126, 78-82.
- Schön, J. (2015). *Basic Well Logging and Formation Evaluation*.
- Sharma, O., & Arya, O. Formation Strength Estimation From Well Log Data For Sand Cut Analysis in Tapti–Daman Area, Western Offshore Basin, India.

Ślota-Valim, M. (2013). Seismic and well log data as a source for the calculation of elastic properties of rock media—conditioning for successful exploration, well trajectory, completion and production design of unconventional reservoirs. *Nafta-Gaz*, 69(8), 583--587.

Ślota-Valim, M. (2015). Static and dynamic elastic properties, the cause of the difference and conversion methods—case study. *Nafta-Gaz*, 11, 816-826.

Wang, Z., & Nur, A. (2000). Seismic and acoustic velocities in reservoir rocks, vol. 3. Recent Developments, Geophysics reprints series, 19, 8-23.

Xu, H., Zhou, W., Xie, R., Da, L., Xiao, C., Shan, Y., & Zhang, H. (2016). Characterization of rock mechanical properties using lab tests and numerical interpretation model of well logs. *Mathematical Problems in Engineering*, 2016.

Zhang, J. J., & Bentley, L. R. (2005). Factors determining Poisson's ratio. *CREWES Research Report*, 17, 1-15.